

ESTIMATION OF FATIGUE CRACK
PROPAGATION LIFE IN BUTT WELDMENTS

by

F. V. Lawrence

P. C. Mainali

A. Y. C. Wong

Department of Civil Engineering

ABSTRACT

A method for calculating the fatigue crack propagation portion of the fatigue life of welds initiating fatigue failure at the toe of the weld is presented. The method can be applied to arbitrarily shaped and loaded members having external fatigue cracks of an assumed initial size. The results indicate that estimates using this procedure can provide reasonable estimates of the fatigue life of mild constructional steels. In the higher strength quenched and tempered steels, however, the initiation period which is neglected in this analysis may constitute the major portion of the fatigue life. The analytical model does allow the relative influence of weld geometry on the crack propagation portion of the fatigue life to be assessed.

A Report of the
FRACTURE CONTROL PROGRAM

College of Engineering, University of Illinois
Urbana, Illinois
October, 1972

TABLE OF CONTENTS

Title Page--Abstract	i
Table of Contents.	ii
List of Symbols.	iii
1. Introduction	
1.1 Crack Initiation and Propagation.	1
1.2 Fatigue in Butt Weldments with Reinforcement Intact	2
2. Procedures	
2.1 Elastic Superposition Approach.	3
2.2 Stress Analysis Using Finite Element Techniques	4
2.3 Stress Intensity Factors for Edge Cracks.	6
2.4 Estimation of Fatigue Crack Propagation Life, N_p	7
3. Results and Discussion	
3.1 Effect of Weld Reinforcement Geometry on N_p	8
3.2 Effect of Material Properties on N_p	8
3.3 Effect of Assumed Flaw Size on N_p	9
3.4 Comparison with Fatigue Test Data	9
4. Conclusions.	11
5. Acknowledgements	12
6. References	13
Tables	15
Figures	17

LIST OF SYMBOLS USED

$\frac{da}{dN}$	crack advance per cycle (in/cycle)
K	stress intensity factor
K_{1C}	critical stress intensity factor
ΔK	range in stress intensity factor (ksi/ $\sqrt{\text{in.}}$)
C, n	crack propagation material properties constants (kip, inch units)
N_p	crack propagation fatigue life (cycles)
a	crack length
a_0	initial crack length
a_f	final crack length
Δa	finite advance of crack
h	height of weld reinforcement
w	width of weld reinforcement
t	plate thickness
Θ	flank angle of the weld
Φ	edge preparation angle of the weld
K_t	stress concentration factor
S	maximum applied tensile stress (stress cycle 0-S)
σ	stress along crack interface
b_0, b_1, b_2, b_3, b_4	constants in stress polynomial
x	coordinate from toe of weld

1. INTRODUCTION

1.1 Crack Initiation and Propagation

The fatigue resistance of a weld is usually less than that of the metal which it joins. This fact can be attributed to several types of discontinuities--geometrical discontinuities, internal flaws, or metallurgical discontinuities--which serve as stress concentrators and accelerate fatigue damage in their locality [9,15].

The fatigue life of a weldment may be considered as consisting of two periods: the number of cycles required to initiate a fatigue crack or to initiate a fatigue crack from a preexisting flaw (initiation), and the number of cycles required to propagate the crack until failure occurs (propagation). The initiation period [3,13] is difficult to measure or predict. The length of this period depends upon the cyclic stress-strain behavior of the material, stress history, residual stresses, and the geometry of the defect.

In welded joints which often contain sizable discontinuities unavoidably created during fabrication, it is often assumed that the initiation period is short relative to the crack propagation period. The fatigue crack propagation portion of the fatigue life is a predictable quantity if the rate of fatigue crack growth per cycle (da/dN) as a function of the range in stress intensity factor (ΔK) has been empirically established for the environment, materials, and loading history in question [1, 2, 10]. Under most conditions of testing there is a threshold level of ΔK , ΔK_{th} , which is just sufficient to propagate the crack. At very high values of ΔK , the crack growth rate becomes infinite, i.e.,

fracture occurs when the peak value of K during a cycle equals K_{1c} . Between these two extremes and particularly for low ΔK values, the measured rates of crack growth can be expressed as a power of the range in stress intensity.

$$\frac{da}{dN} = C(\Delta K)^n \quad (1)$$

From Eq. 1, the crack propagation period of the fatigue life can be estimated.

$$N_p = \int_{a_0}^{a_f} \frac{1}{C(\Delta K)^n} da \quad (2)$$

If Eq. 2 proves impossible to obtain in a closed form, the integral may be evaluated by finite difference techniques.

$$N_p = \sum_{a_0}^{a_f} \frac{1}{C(\Delta K)^n} \Delta a \quad (3)$$

In previous studies [3,8] the author has used Eq. 3 to estimate the fatigue crack propagation life of welds containing internal discontinuities. In the present study, the fatigue crack propagation life has been estimated for butt weldments containing external flaws (toe cracks) using an elastic superposition procedure and Eq. 3.

1.2 Fatigue in Butt Welds with Reinforcement Intact

Butt weldments tested in fatigue with their reinforcement intact exhibit less fatigue resistance than plain plate or butt welds with their reinforcement removed due to the notch associated with the toe of the

weld [15]. Fatigue cracks invariably initiate at these locations (shown schematically in Fig. 1) and propagate through the heat affected zone and base metal in a direction perpendicular to the applied stress.

The height of the reinforcement (h), the width of the reinforcement (w), and the thickness of the weld (t) influence the severity of this notch. If one considers the weld reinforcement to be a segment of a circle, the ratios h/w and w/t determine the geometry, or, alternatively, the geometry may be specified by the flank angle (θ) and the edge preparation angle (ϕ): see Fig. 1. The ratios h/w and w/t are functions of θ and ϕ respectively.

$$\frac{h}{w} = \frac{1}{2} \tan \frac{\theta}{2} \quad (4)$$

$$\frac{w}{t} = \tan \frac{\phi}{2} \quad (5)$$

The geometry of the weld will influence the state of stress along the direction of fatigue crack propagation and hence influence the rate of crack growth and the fatigue crack propagation life of a weldment.

To calculate the fatigue crack propagation lives of double-V butt welds of varying geometry, the following procedure was used.

2. PROCEDURES

2.1 Elastic Superposition

With reference to Fig. 2, one wishes to know the stress intensity factor for an edge crack in a body which is arbitrarily loaded. This condition is represented by the first body in Fig. 2. Using elastic superposition, the state of stress of the first body can be considered to

be the superposition of the stresses in bodies two and three (Fig. 2). In the second body, the crack is held closed by the tractions necessary to do so, so that the body may be considered to be unflawed. The stresses in the second body and in particular the tractions necessary to hold the crack closed may be found using an appropriate elastic solution, or by using approximate finite element methods.

The stresses in the third body which is not loaded externally are due to loading the internal surfaces of the crack with the negative of the tractions found in second body. By superposing the stress fields of the bodies two and three, one obtains the stresses in first body. More importantly for present purposes, the stress intensity factor associated with the crack in third body is identical to that in the first body.

In terms of the present problem, the calculation of the stress intensity factor for an edge notch in a particular geometry double-V butt weld consists of the following steps:

1. Find the tractions in an uncracked weldment along the line to be traversed by the crack, using finite element methods.
2. Fit these stresses with a polynomial function.
3. Calculate the stress intensity factor for any particular length of crack.
4. Use Eq. 3 to obtain the fatigue crack propagation life, N_p .

2.2 Stress Analysis Using Finite Element Techniques

Examples of the geometries studied are shown in Fig. 3. Because of symmetry only one quadrant of the weld need be considered. Geometries having flank angles (θ) of 0, 10, 20, 30, 45, and 60 degrees and edge preparation angles (ϕ) of 30, 45, 60, and 90 degrees were analyzed using

finite element methods. The geometry of a particular weld was modeled by subdividing it into a mesh of interconnected triangles (Fig. 4). Linear strain triangles were used and plane strain conditions were assumed. The applied (tensile) stresses were replaced by equivalent nodal forces. The boundary conditions allowed freedom of displacement along the respective axes, and restraints perpendicular to the axes. The stresses at each node were determined by averaging the stresses of all triangles joined at that node. A finer mesh was necessitated at the toe of the weld where the stress level changes rapidly.

The calculated stress levels for different flank angles are shown in Fig. 5 and listed in Table 1. It can be seen that the maximum value of stress (σ_{\max}) occurs at the toe of the weld and is between 1.2 to 1.8 times larger than the applied stress (S). The stress level decreases rapidly with distance away from the toe of the weld, and after a distance of approximately 0.1t, the stress level (σ) is approximately that of the applied stress (S). At greater distances, the stress is slightly below the applied stress.

The calculated stress concentration factor ($K_t = \frac{\sigma_{\max}}{S}$) is plotted as a function of the geometries studied in Fig. 6. The stress concentration factor increases rapidly with increasing flank angle θ (or h/w ratio) but does not increase much after $\theta = 45^\circ$ (h/w \approx 0.2). For $\theta = 60^\circ$, $\phi = 90^\circ$ a maximum K_t of 1.8 was found. Reducing the angle of the edge preparation, ϕ , reduces the stress concentration markedly: when $\theta = 60^\circ$, $\phi = 30^\circ$, K_t is reduced to 1.27.

The calculated stresses shown in Fig. 5 were fitted with a fourth order polynomial using a least squares fit.

$$\frac{\sigma}{S} = b_0 + b_1\left(\frac{x}{t}\right) + b_2\left(\frac{x}{t}\right)^2 + b_3\left(\frac{x}{t}\right)^3 + b_4\left(\frac{x}{t}\right)^4 \quad (6)$$

where σ = stress at any point x
 S = applied stress
 x = distance from toe of weld
 b_0, b_1, b_2, b_3, b_4 = constants

This analytical expression can be conveniently used for stress intensity factor calculations (Eq. 8).

2.3 Stress Intensity Factor for Edge Cracks

The stress intensity factor for an edge crack in a semi-infinite solid uniformly loaded at a distance from the crack is given approximately by [12,10]:

$$K = 1.1\sigma\sqrt{\pi a} \quad (7)$$

The stress intensity factor for an edge crack in a semi-infinite solid loaded internally by an arbitrary system of stresses has been given by Emery [14,11] (see Fig. 7).

$$K = \sqrt{\pi a} \left\{ 1.1\sigma_a - \int_0^a f\left(\frac{x}{a}\right) \frac{d\sigma}{dx} dx \right\} \quad (8)$$

where a = crack length
 σ_a = stress at crack tip
 and

$$f\left(\frac{x}{a}\right) = 0.8\left(\frac{x}{a}\right) + 0.04\left(\frac{x}{a}\right)^2 + 0.352 \times 10^{-5} e^{11.18\left(\frac{x}{a}\right)}$$

When the stress does not vary along the internal surface of the crack, i.e., $\frac{d\sigma}{dx} = 0$, Eq. 8 reduces to Eq. 7.

Substituting Eq. 8 into Eq. 2 one obtains:

$$N_p = \int_{a_0}^{a_f} \frac{da}{C[\sqrt{\pi a} (1.1\sigma - \int_0^a f(\frac{x}{a}) \frac{d\sigma}{dx} dx)]^n} \quad (9)$$

or in terms of finite differences and Eq. 3,

$$N_p = \sum_{a_0}^{a_f} \frac{\Delta a}{C[\sqrt{\pi a} (1.1\sigma - \sum_0^a f(\frac{x}{a}) \frac{d\sigma}{dx} \Delta x)]^n} \quad (10)$$

2.4 Estimation of Fatigue Crack Propagation Life, N_p

Since the variation of stress along the interface to be traversed by the toe crack is a known function of distance (Eq. 6), ΔK , the range in stress intensity can be calculated for any crack length (a) and the fatigue crack propagation life calculated by Eq. 10. The exact computation procedure is diagrammed in Fig. 8 and a FORTRAN program statement is listed in Fig. 9. Both of the summations are performed using an open-ended form of Simpson's Rule for numerical integration. The use of Simpson's Rule was found to give results within 1 percent of closed form solutions (found by substituting Eq. 7 into Eq. 2)* when the increment in crack size was 0.01 inches.

In the calculations performed, the plate size of the weld (t) was assumed to be one inch for the purpose of comparing the calculations with available test results. The final flaw size was chosen to be 0.2 inches or 0.2t. This choice avoids the necessity of correcting for the opposite free surface of the plate. The fatigue life spent in propagating the remaining plate thickness is small compared with the life spent in propagating to a length of 0.2 inches. Further, for most practical purposes a flaw size of 0.2t can be considered as constituting failure.

*This comparison is valid when $\theta = 0$.

3. RESULTS AND DISCUSSION

3.1 Effect of Weld Reinforcement Geometry on N_p

The calculated growth of a 0.01 in. toe crack in a one-inch thick double-V butt weldment subjected to zero-tension load cycling is shown in Fig. 10. The material is assumed to be a ferrite-pearlite steel having C and n values of 0.36×10^{-9} and 3.0, respectively [17].

Increasing the flank angle of the weld (θ) from zero to 20 degrees greatly accelerates the rate of crack growth [6,16]. Increases in flank angle beyond 30 degrees have little further effect. The major period of a crack's fatigue life is spent at very small crack lengths.

The calculated influence of flank angle θ , and edge preparation angle ϕ upon N_p is shown in Fig. 11. Decreasing ϕ or decreasing the width of the weld (w) for a given thickness lengthens the fatigue crack propagation life. Small reductions in ϕ are equivalent to very large reductions in θ when θ is larger than 15 degrees.

3.2 Effect of Material Properties on N_p

The effect of varying material properties is shown in Fig. 12 in which the calculated fatigue life N_p is compared for ferrite-pearlite and martensitic steels. Average C and n values for martensitic steels are 0.66×10^{-8} and 2.25 respectively [17]. These values yield N_p values for martensitic steels which are approximately one-third those of ferrite-pearlite steels for the initial flaw size chosen ($a_0 = 0.01$ inch). The reduction in N_p with increasing θ is less pronounced in this material.

These effects can also be seen in the S-N plots of Fig. 13. The slope of the S-N curve is equal to the reciprocal of the exponent (n) in

Eq. 1. An initial flaw size of 0.01 inch is assumed in this plot. Ferrite-pearlite steels exhibit longer lives and more sensitivity to the weld reinforcement geometry than the martensitic steels. The difference between the predicted lives for the two steels diminishes with increasing stress level.

3.3 Effect of Assumed Initial Flaw Size on N_p

In addition to the values of C , n , stress level, and geometry, the computed fatigue crack propagation life is extremely sensitive, if not the most sensitive, to the assumed initial flaw size. The sensitivity of the results is demonstrated in Fig. 14. The proper assumption of initial flaw size is critical for accurate predictions of N_p , and at present one can only guess at the appropriate value. Most calculations in this work have been carried out with an assumed crack size of 0.01 inch. This is a reasonably sized "small" crack which will most certainly exist at some (early) stage in the fatigue life of a weld. Assuming smaller cracks (0.001 inch) poses no problems for the analytical procedures described, but the behavior of such small cracks may not be properly described by the power law (Eq. 1). Nonetheless, crack propagation lives N_p have been plotted for flaw sizes of 0.1, 0.01, and 0.001 inch.

3.4 Comparison With Fatigue Test Data

The predicted fatigue crack propagation lives are compared with the total fatigue lives of constructional grade ferritic-pearlitic steels (A36 and A441) in Fig. 16 and constructional grade low-alloy martensitic steels (HY-130, HY-100 and T1) in Fig. 15. Naturally, this comparison is strained because any period spent in crack initiation is ignored. On the

other hand, several current investigators have asserted that the initiation period in welds failing at the toe of the weld is negligibly short.

The data for the A36 and A441 [6] are in quite good agreement with the predicted fatigue crack propagation life. The spread in the test data is due to controlled variations and weld reinforcement geometry. The predicted fatigue crack propagation life should be compared with test specimens giving the longest lives since these are of equivalent geometries. On this basis, it seems that initial flaw size assumptions of 0.01 inch and 0.001 inch bound the test data. For the A36 and A441 steel data, the major portion of the fatigue life can be explained on the basis of fatigue crack propagation alone, with the assumption of a reasonable initial flaw size between 0.01 and 0.001 inches. This, however, is not the case with the data for the martensitic steels [4, 5, 7]. The large difference between the predicted crack propagation life and measured total fatigue life implies that a major portion of the fatigue life is spent in initiation. Assuming an initial crack size smaller than 0.001 inch would seem unreasonable and beyond the range of applicability of the power law (Eq. 1). Although the crack propagation life of the martensitic steels is shorter (for the condition at hand), the longer (apparent) initiation period contributes to the life of these specimens so that there is little difference between the fatigue life of the martensitic steel weldments and the ferritic-pearlitic weldments which exhibit longer crack propagation lives but lesser initiation periods.

The effects of weld geometry upon the fatigue lives of the A36 and A441 fatigue specimens [6] is shown for two different stress levels in Figs. 17 and 18, respectively. Again, the data are bounded by the

calculated fatigue crack propagation lives for assumed initial crack sizes of 0.01 and 0.001 inches. As the flank angle, θ , or height to width ratio, h/w , is reduced the total fatigue lives of the tested specimen increase more rapidly than expected, at the higher stress levels. Possibly, the initiation period becomes proportionally larger as the severity of the stress at the toe of the weld is reduced.

4. CONCLUSIONS

An analytical model has been developed to calculate the fatigue crack propagation life of arbitrarily shaped and loaded weldments containing external crack of an assumed initial size.

With the model the effects of weld geometry, material properties, stress level, and initial flaw size were considered. Differences in weld geometry were found to influence the fatigue crack propagation life by as much as a factor of three while material properties and initial flaw size can have a much larger effect.

Comparisons with fatigue results for A36 and A441 steel weldments reveal a good agreement between the calculated fatigue crack propagation lives and the total lives of tested specimens implying that in these materials the crack initiation period is relatively short. In such cases the calculation methods discussed can provide a reasonable lower bound for the fatigue life of such materials. There is a large discrepancy between the test results for low-alloy martensitic steels and the calculated fatigue crack propagation lives using similar assumptions of initial crack sizes, which implies that a larger proportion of the fatigue life is spent in crack initiation in these materials.

Although the uncertainty as to the proper choice of initial flaw size prohibits the exact calculation of the fatigue crack propagation life, comparisons of calculated lives for differing geometries with identical initial crack sizes does allow the influence of geometry on the fatigue crack propagation life to be studied.

5. ACKNOWLEDGEMENTS

The support of the Fracture Control Program during the major part of this investigation is gratefully acknowledged. The authors wish to thank J. P. Gallagher currently associated with Experimental Mechanics Structures Division, Flight Dynamics Laboratory, Wright-Patterson Air Force Base, for his helpful comments and advice.

6. REFERENCES

1. Paris, P. C. and Erdogan, F., "A Critical Analysis of Crack Propagation Laws," Journal of Basic Engineering, ASME Transactions, Vol. 85, Series D, No. 4, 1963, p. 528.
2. Barsom, V. M., Imhof, E. J., Jr., and Rolfe, S. T., "Fatigue Crack Propagation in High Strength Steels," U. S. Steel Technical Report 39-018-007(27), December 20, 1968.
3. Lawrence, F. V., Jr. and Radziminski, "Fatigue Crack Initiation and Propagation in High-Yield-Strength Steel Weld Metals," Welding Journal, Vol. 49, No. 10, October 1970.
4. Radziminski, J. B., Lawrence, F. V., Jr., Mukai, S., Panjwani, P. N., Johnson, R., Mah, R. and Munse, W. H., "Low Cycle Fatigue of HY-130(T) Butt Welds," Civil Engineering Studies, Structural Research Series, No. 342, University of Illinois, December 1968.
5. Radziminski, J. B., Lawrence, F. V., Jr., Wells, T. W., Mah, R. and Munse, W. H., "Low cycle fatigue of Butt Weldments of HY-100(T) and HY-130(T) Steels," Civil Engineering Studies, Structural Research Series, No. 301, University of Illinois, July 1970.
6. Williams, H. E., Ottsen, H., Lawrence, F. V., Jr., and Munse, W. H., "The Effect of Weld Geometry on the Fatigue Behavior of Welded Connections," Civil Engineering Studies, Structural Research Series, No. 366, University of Illinois, August 1970.
7. Munse, W. H., Stallmeyer, J. E. and Bruckner, W. H., "Fatigue Behavior of Plain Plate and Butt-Welded Joints in T-1 Steel and T-1A Steel," A report of an investigation conducted for the U. S. Steel Corporation, University of Illinois, January 1966.
8. Lawrence, F. V., Jr. and Munse, W. H., "Fatigue Crack Propagation in Steel Weldments," Automotive Engineering Congress, Detroit, Michigan, No. 720267, January 10-14, 1972.
9. Fisher, J. W., Frank, K. H., Hert, M. A. and McNamer, B. M., "Effect of Weldment on the Fatigue Strength of Steel Beams," Fritz Engineering Laboratory, Department of Civil Engineering, Lehigh University, September 1969.
10. Miller, G. A., "The Dependence of Fatigue Crack Growth Rate on the Stress Intensity Factor and the Mechanical Properties of Some High Strength Steels," Transactions ASM, Vol 61, 1968.

11. Emery, A. F. and Walker, G. E., Jr., "Stress Intensity Factor for Edge Cracks in Rectangular Plates with Arbitrary Loadings," ASME Publication 68-WA/MET-18 presented at ASME Winter Annual Meeting and Energy Systems Exposition, New York, December 1-5, 1968.
12. Paris, P. C. and Sih, G. C., "Stress Analysis of Cracks," ASTM Report STP-381, 1966.
13. Iida, K., "Crack Initiation Life in Low Cycle Fatigue," Department of Naval Architecture, University of Tokyo, NAUT Report, No. 9003, April 1972.
14. Emery, A. F., "Stress Intensity Factors for Thermal Stress in Thick Hollow Cylinders," Journal of Basic Engineering, March 1966.
15. Gurney, T. A., "Fatigue of Welded Structures," Cambridge University Press, 1968.
16. Sanders, W. W., Jr., Derecho, A. T. and Munse, W. H., "Effect of External Geometry on Fatigue Behavior of Welded Joints," Civil Engineering Studies, Structural Research Series, No. 290, University of Illinois, May 1965.
17. Barsom, J. M., "Fatigue-Crack Propagation in Steels of Various Yield Strengths," Paper presented at First National Congress on Pressure Vessels and Piping, San Francisco, May 1971.

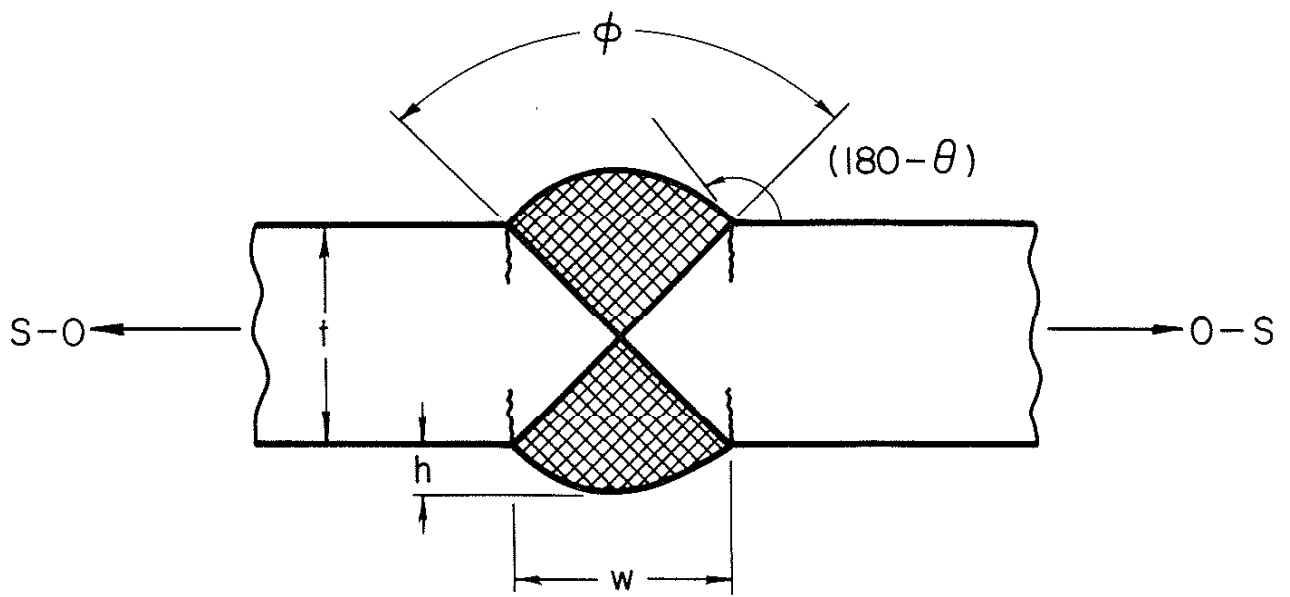
TABLE 1

Stress Concentration Factors for Various Geometries

θ	$\frac{h}{w}$	STRESS CONCENTRATION FACTORS (K_t)			
		$\phi = 90^\circ$ w/t = 1.0	$\phi = 60^\circ$ w/t = 0.58	$\phi = 45^\circ$ w/t = 0.40	$\phi = 30^\circ$ w/t = 0.27
0°	0.0	1.0	1.0	1.0	1.0
10°	0.045	1.36	1.26	1.18	1.10
20°	0.088	1.56	1.42	1.25	1.20
30°	0.134	1.77	1.54	1.34	1.24
45°	0.207	1.83	1.62	1.38	1.28
60°	0.29	1.82	1.63	1.38	1.27

Results of Stress Analysis for Various Weld Profiles

θ	$\frac{h}{w}$	ϕ	$\frac{w}{L}$	b_0	b_1	b_2	b_3	b_4
0	0	90°	1.0	1.0	0.0	0.0	0.0	0.0
10	0.045	"	"	1.3643	-7.0907	42.838	-104.20	87.525
20	0.088	"	"	1.5631	-10.9766	66.255	-161.048	135.20
30	0.134	"	"	1.7168	-14.0275	84.724	-205.972	172.92
45	0.207	"	"	1.8311	-16.5662	100.538	-244.876	2-5.745
60	0.29	"	"	1.8192	-16.3804	99.002	-240.467	201.652
0.	0.0	60°	0.58	1.0	0.0	0.0	0.0	0.0
10	0.045	"	"	1.2608	-5.4106	33.452	-81.736	68.659
20	0.088	"	"	1.4193	-8.7313	53.981	-131.818	110.665
30	0.134	"	"	1.5367	-11.3389	70.551	-174.845	145.378
45	0.207	"	"	1.6183	-13.272	82.985	-203.737	171.545
60	0.29	"	"	1.6342	-13.8398	86.995	-214.146	180.583
0	0.0	45°	0.40	1.0	0.0	0.0	0.0	0.0
10	0.045	"	"	1.1812	-4.125	26.509	-65.865	55.785
20	0.088	"	"	1.2543	-5.8365	37.533	-93.23	78.937
30	0.134	"	"	1.3379	-7.9347	51.605	-129.039	109.723
45	0.207	"	"	1.3826	-9.2857	61.650	-156.326	134.234
60	0.29	"	"	1.3826	-9.5617	64.0263	-162.986	140.255
0	0.0	30°	0.27	1.0	0.0	0.0	0.0	0.0
10	0.045	"	"	1.0977	-2.4068	16.061	-40.651	34.782
20	0.088	"	"	1.2048	-5.1746	34.914	-88.922	76.386
30	0.134	"	"	1.2408	-6.1639	41.778	-106.646	91.737
45	0.207	"	"	1.2798	-7.4016	50.766	-130.398	112.597
60	0.29	"	"	1.2717	-7.4558	51.629	-133.236	115.385



$$h/w = 1/2 \tan \theta/2$$

$$w/t = \tan \phi/2$$

Fig. 1 Geometry of a Double-V Butt Weldment

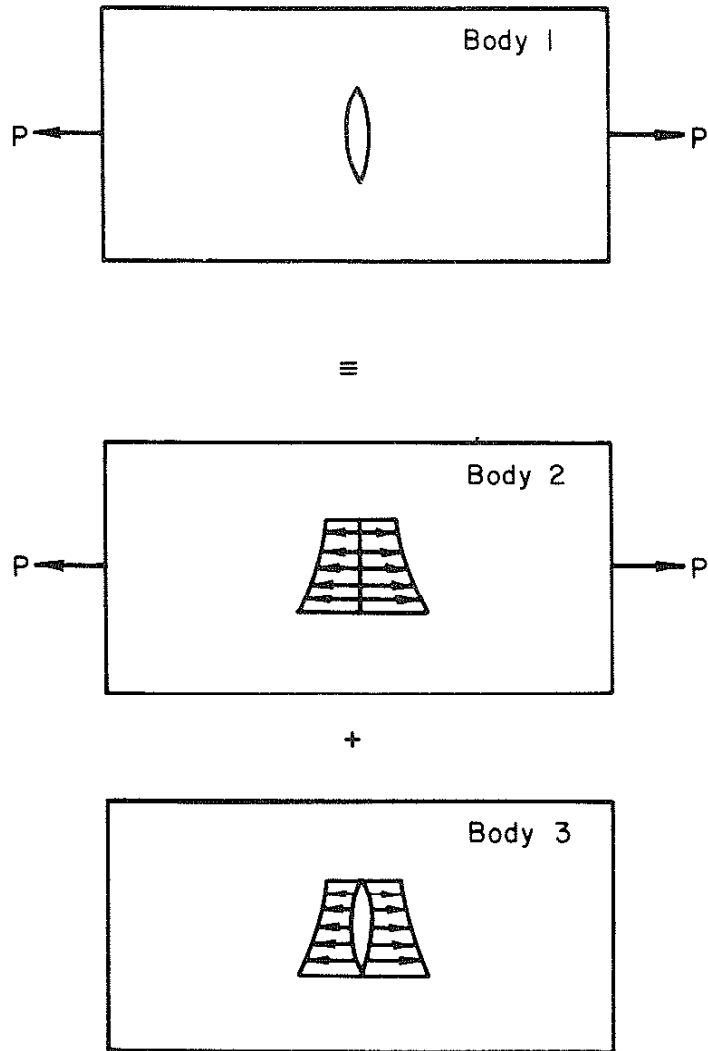
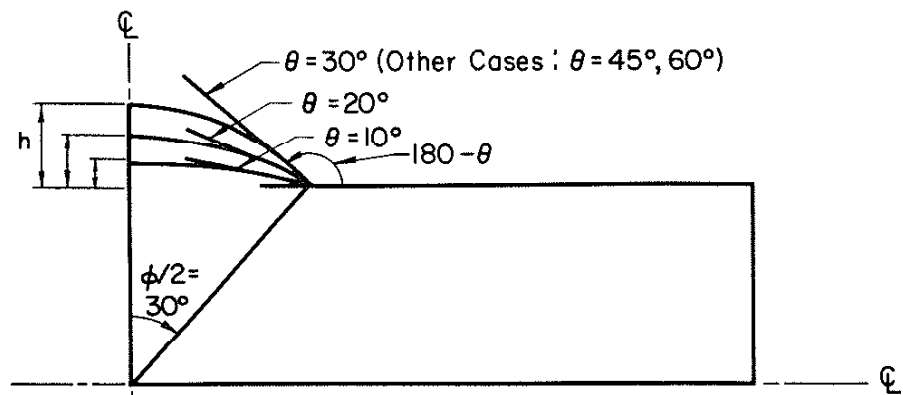
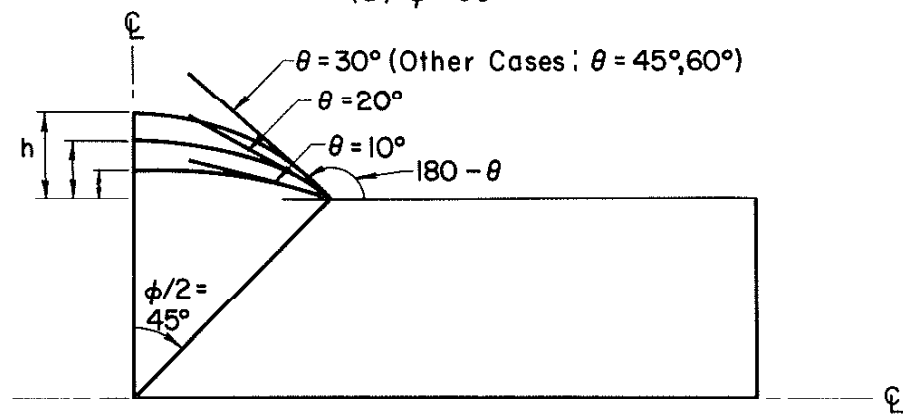


Fig. 2 Superposition Principle for Stresses in a Flawed Body



(a) $\phi = 60^\circ$



(b) $\phi = 90^\circ$

Fig. 3 Geometry of Idealized Weldments

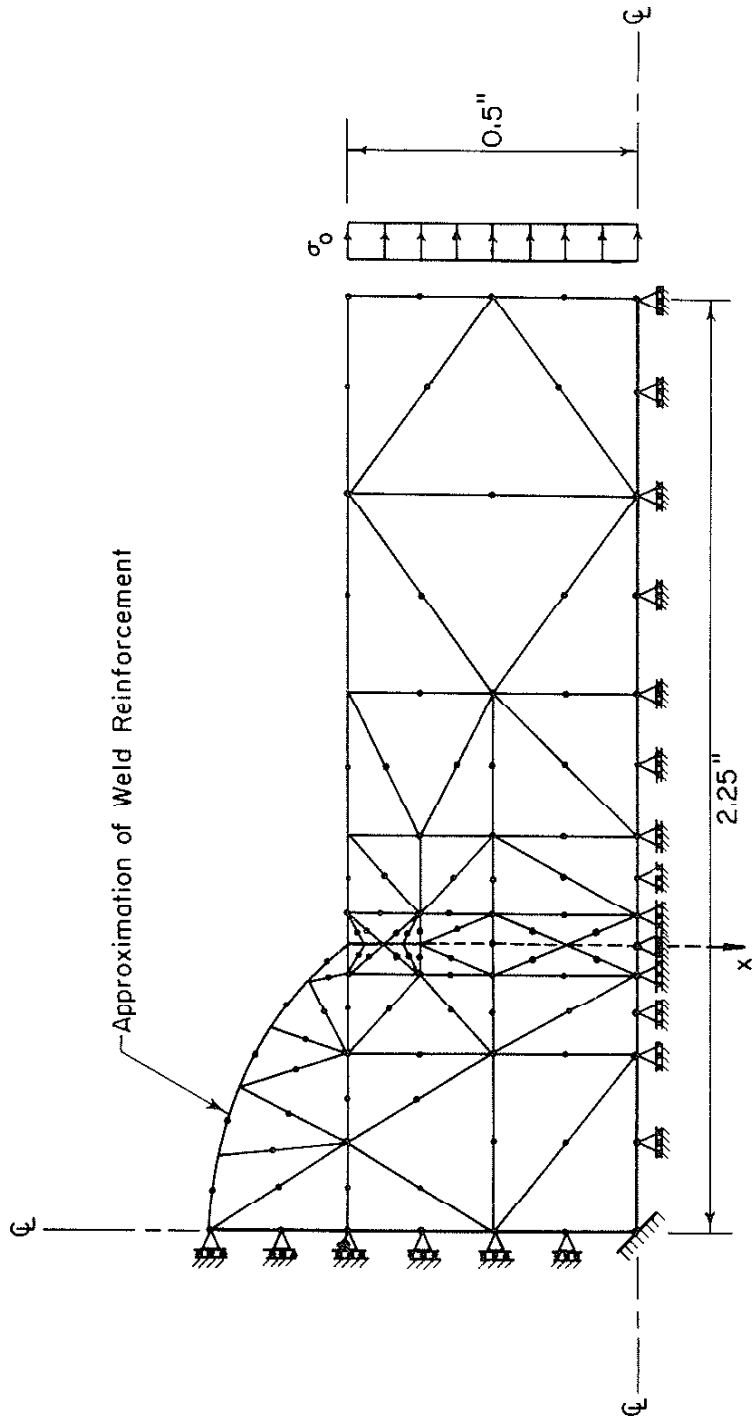


Fig. 4 Finite Element Network for Stress Analysis

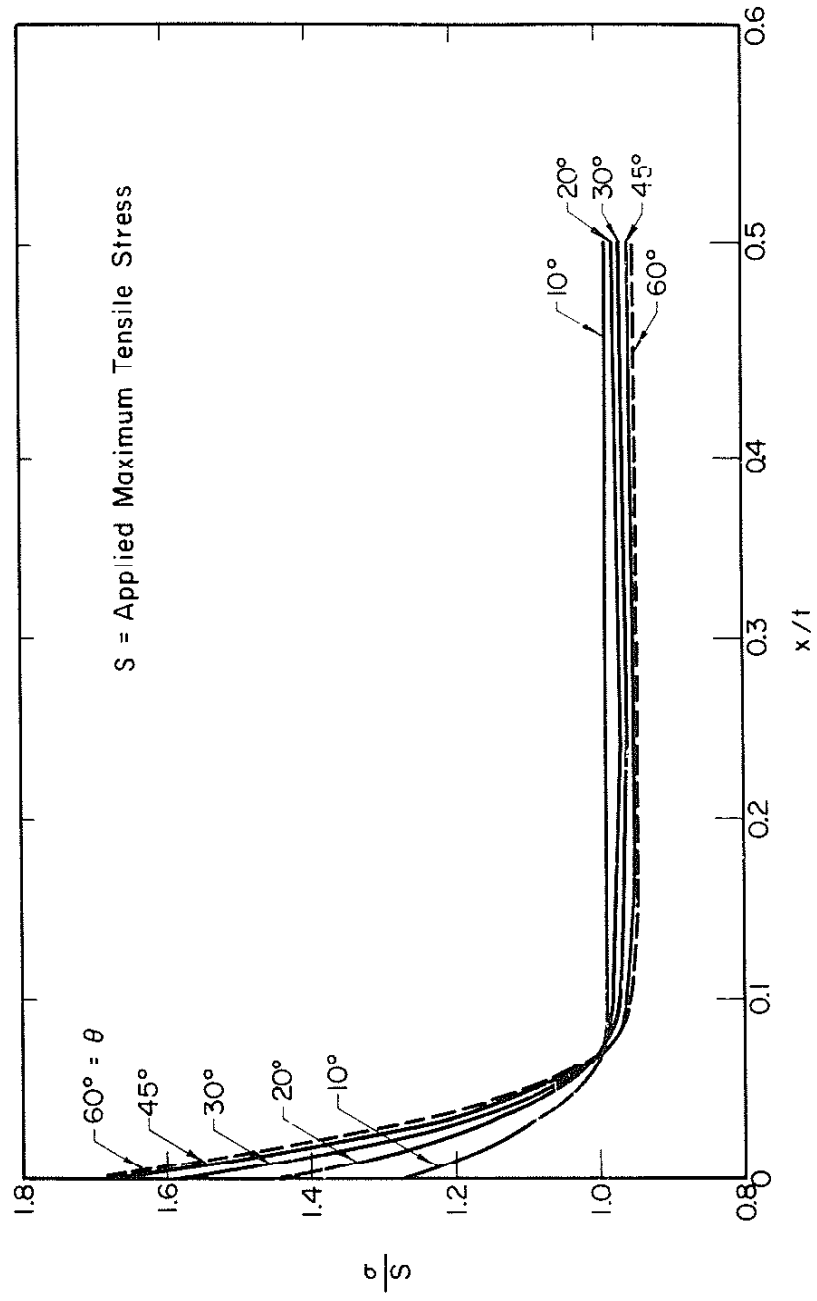


Fig. 5 Stress Variation Inward from the Toe of the Weld Reinforcement

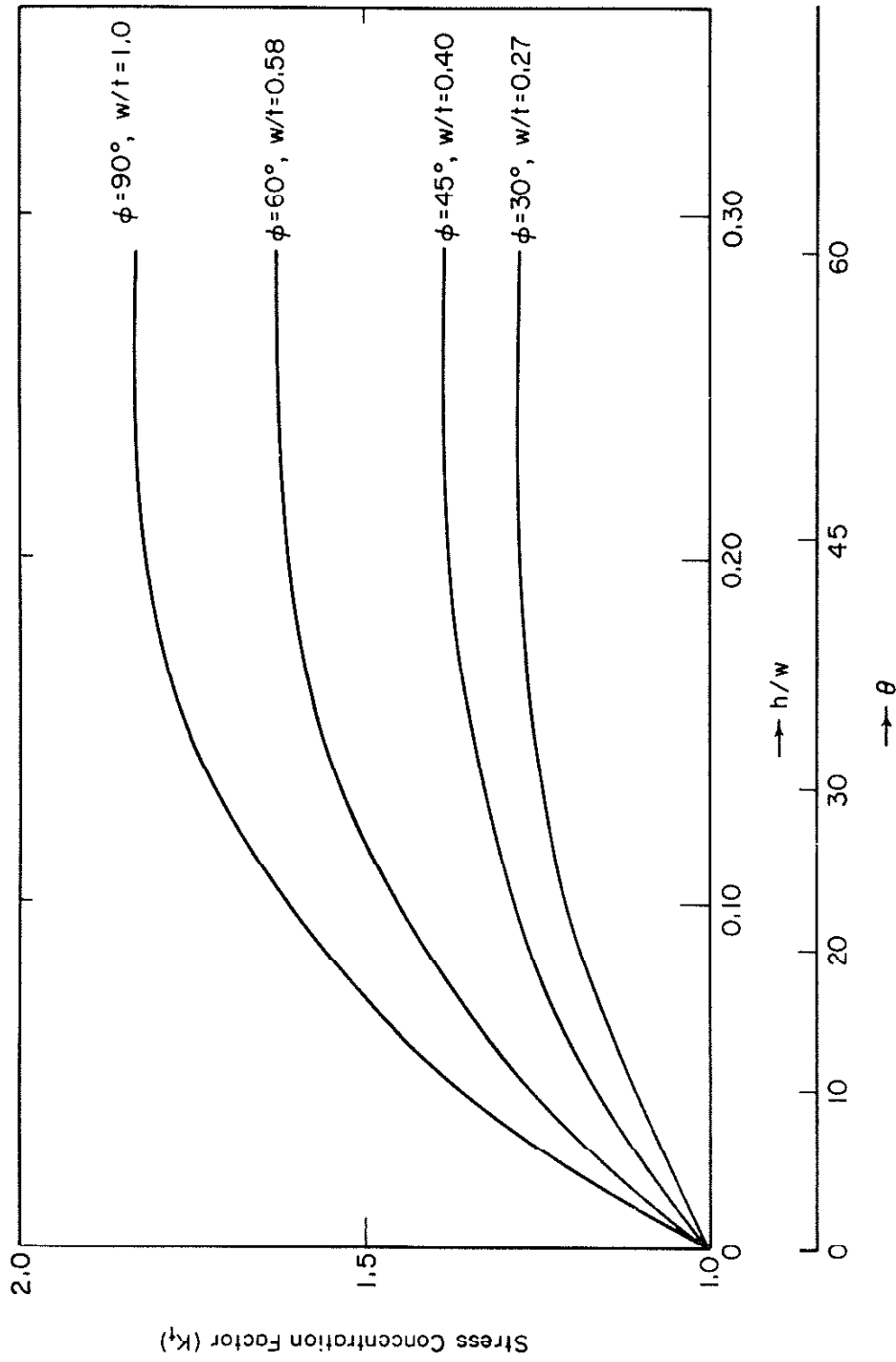
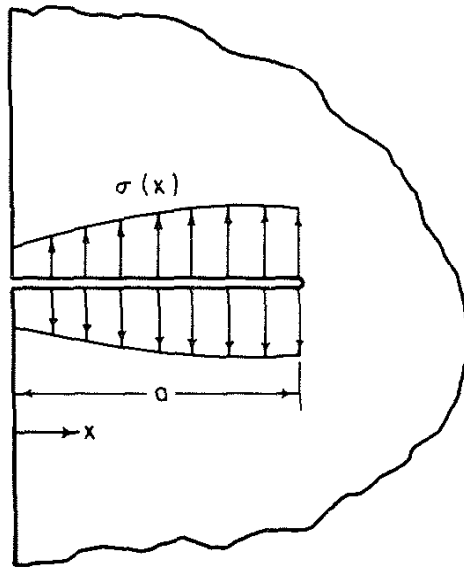


Fig. 6 Stress Concentration Factor for Various Weld Reinforcement Geometries



$$K = \sqrt{\pi a} \left\{ 1.1 \sigma - \int f\left(\frac{x}{a}\right) \cdot \frac{d\sigma}{dx} dx \right\}$$

$$f\left(\frac{x}{a}\right) = 0.8\left(\frac{x}{a}\right) + 0.04\left(\frac{x}{a}\right)^2 + 3.62 \times 10^{-6} \times e^{11.18\left(\frac{x}{a}\right)}$$

Fig. 7 Stress Intensity Factor for an Edge Crack Loaded with an Arbitrary System of Internal Stresses

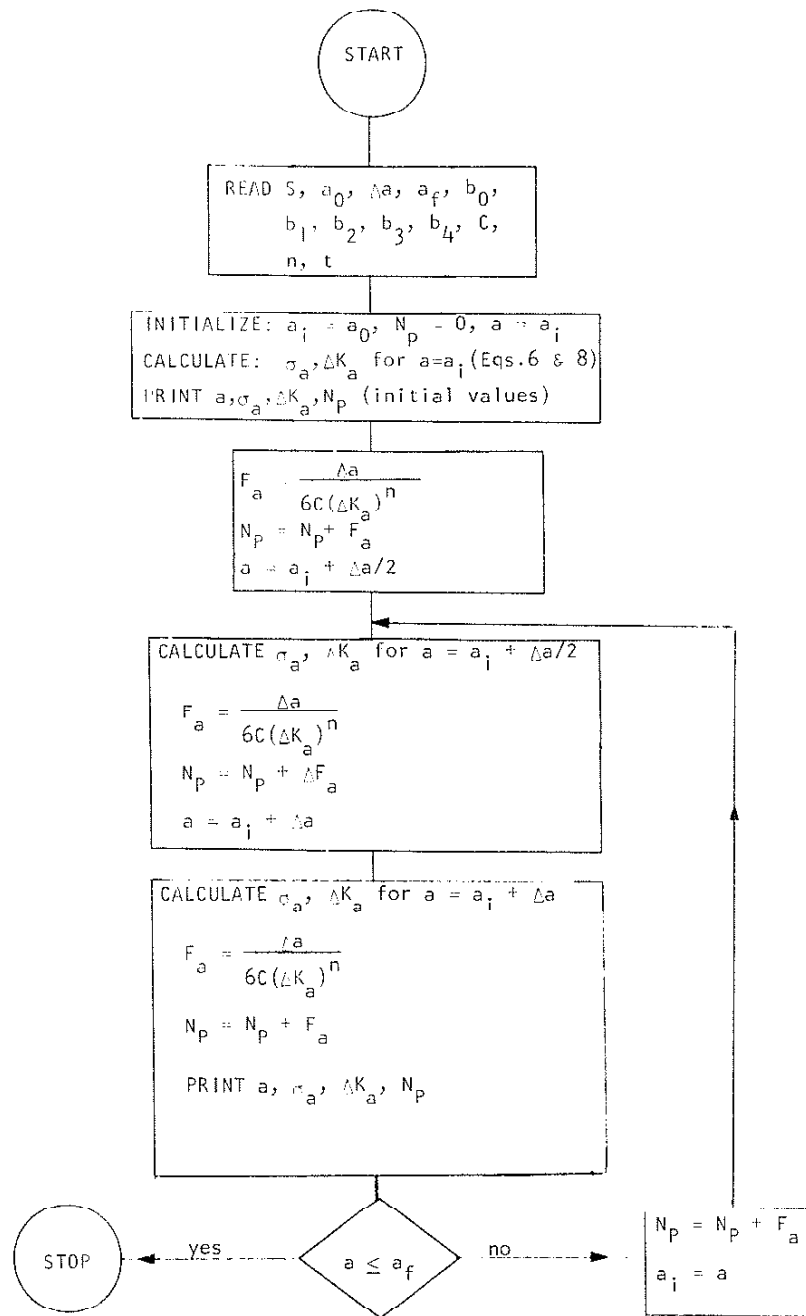


Fig. 8 Flow Chart for Determining Fatigue Crack Propagation Life, N_p

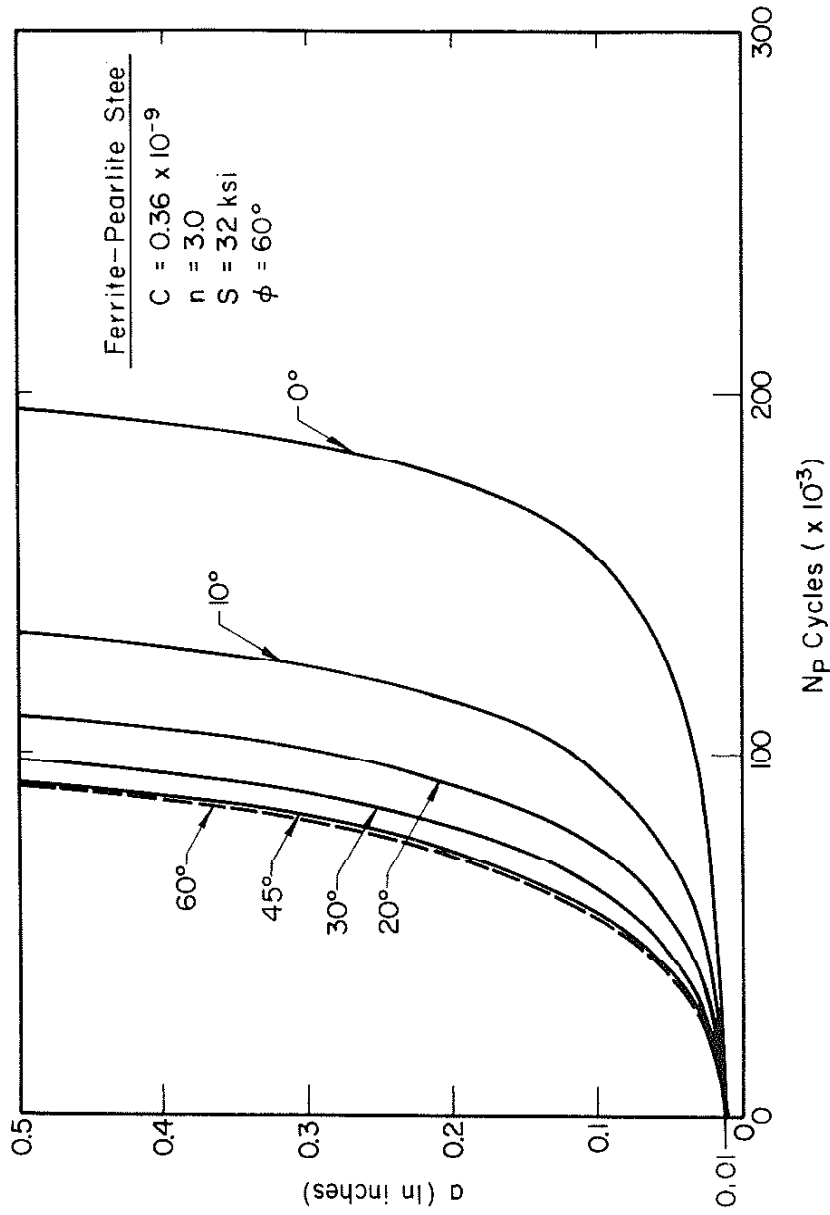


Fig. 10 Variation in Δ_p with Change in Flank Angle, ϕ

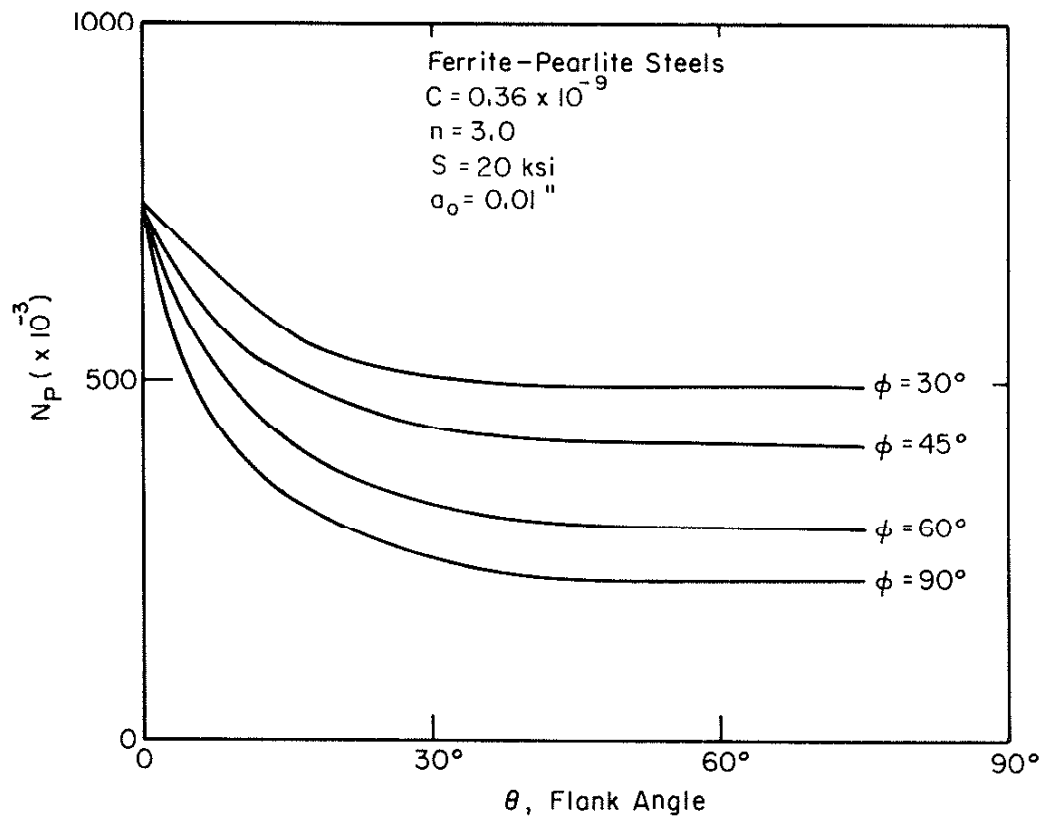


Fig. 11 Variation in N_p with Change in Edge Preparation Angle, ϕ

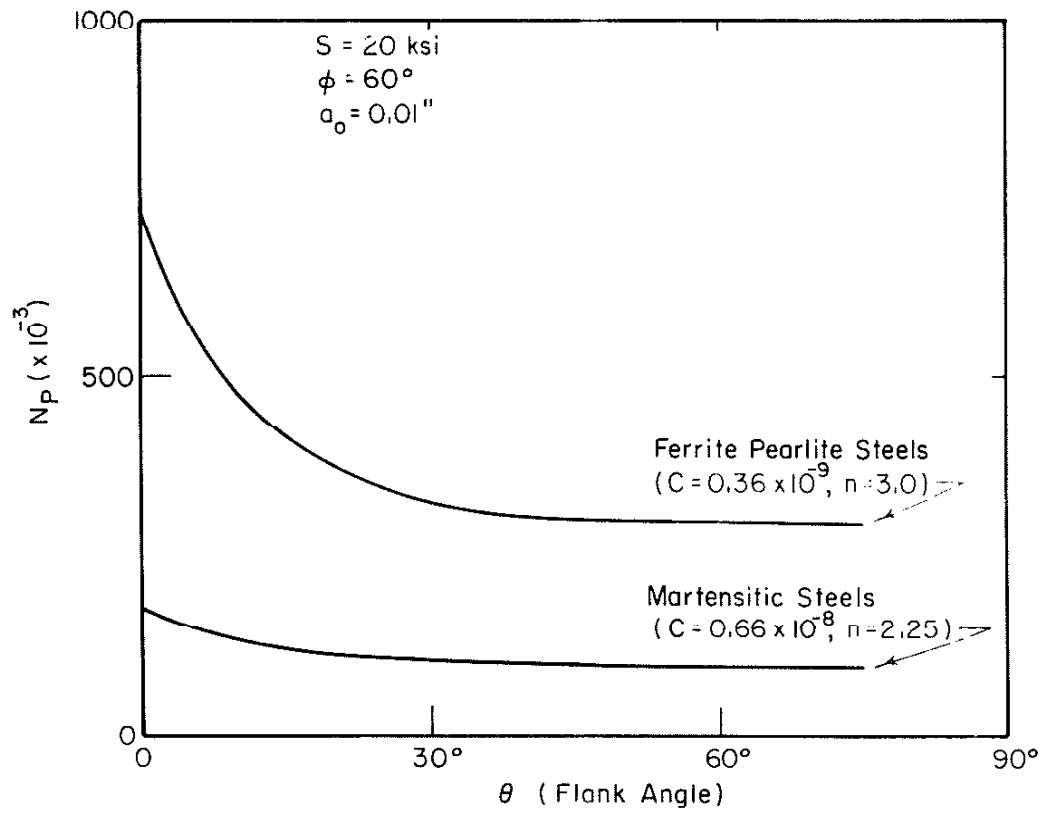
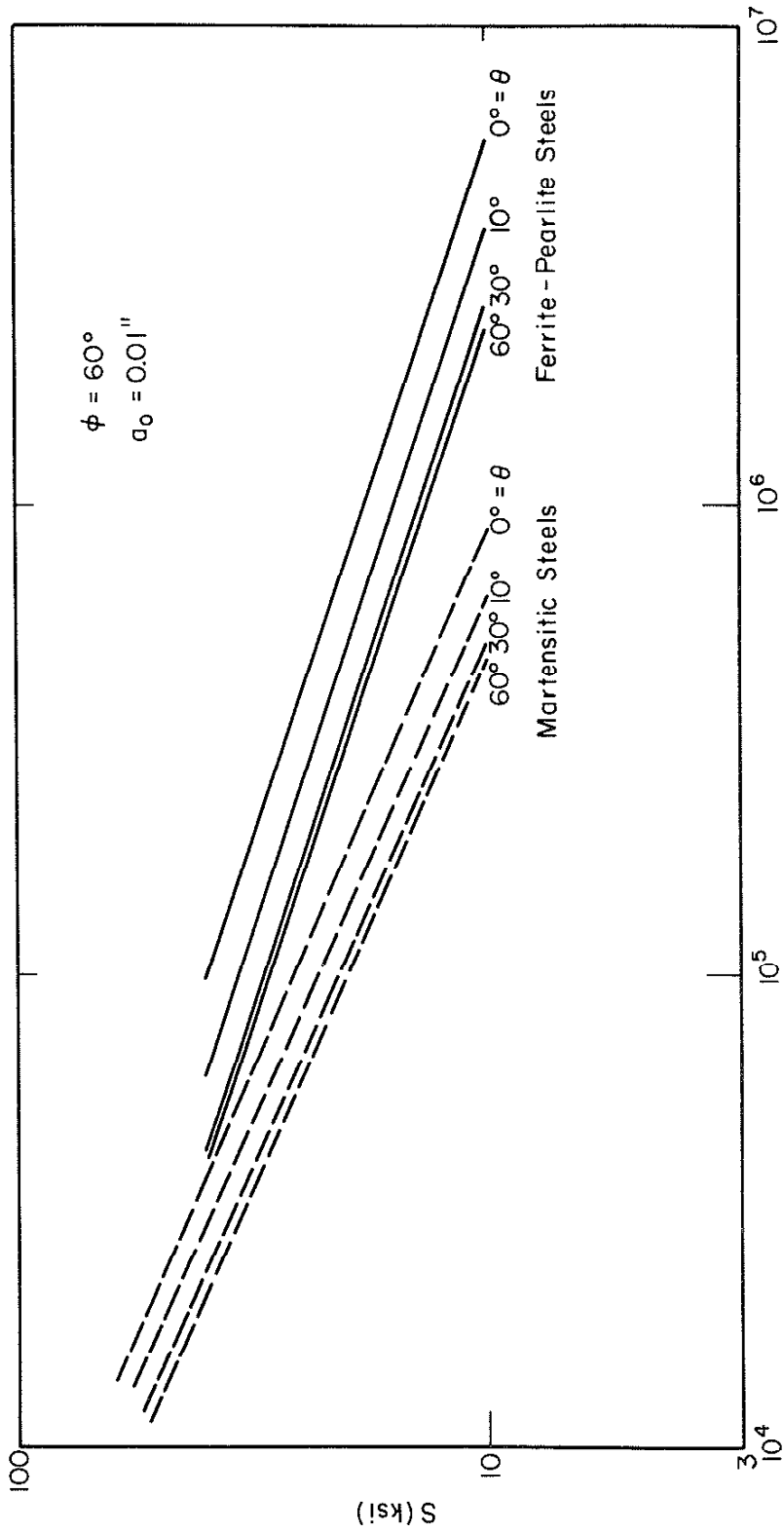


Fig 12 Effect of Varying Material Properties on N_p



N_p , Cycles

Fig. 13 S - N_p Plot for Martensitic and Ferrite-Pearlite Steels

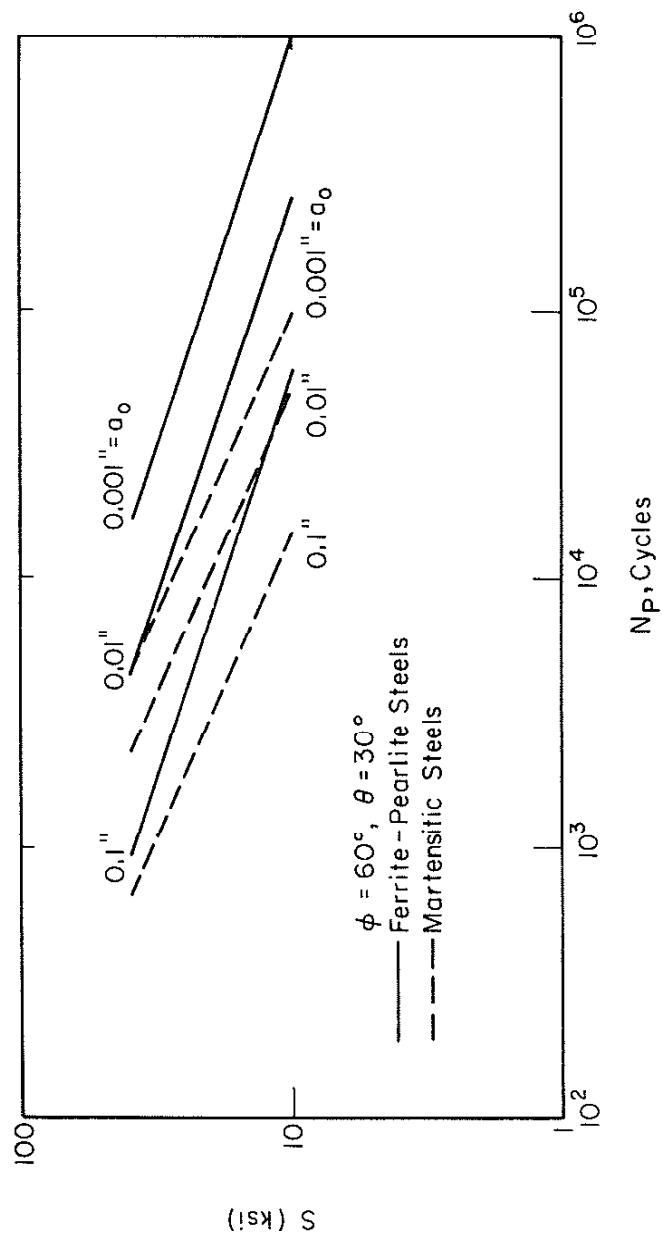


Fig. 14 Effect of Initial Flaw Size, a_0 , on Fatigue Crack Propagation Life, N_p

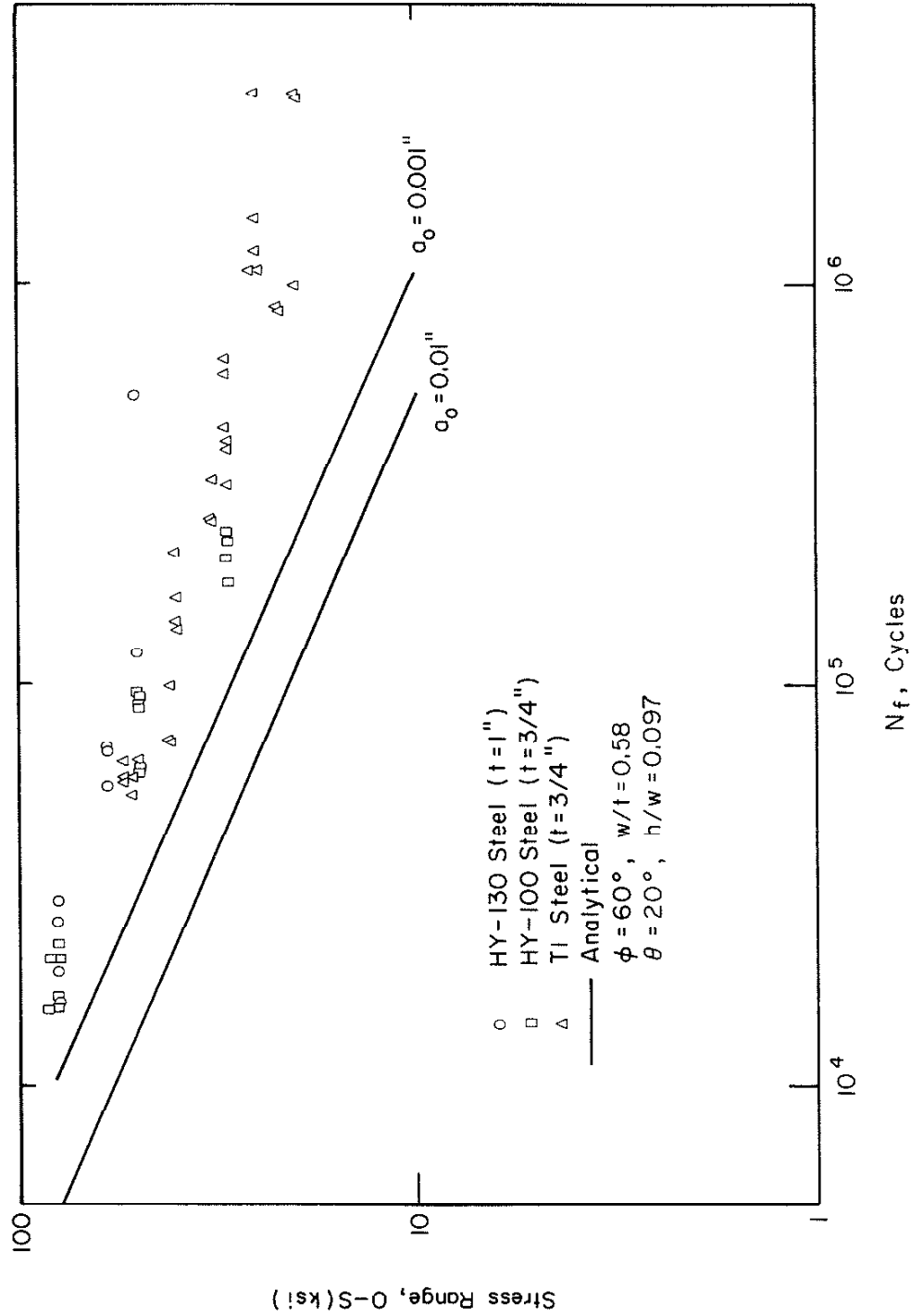


Fig. 15 Comparison of Analytical and Test Results for N_f for Martensitic Steels

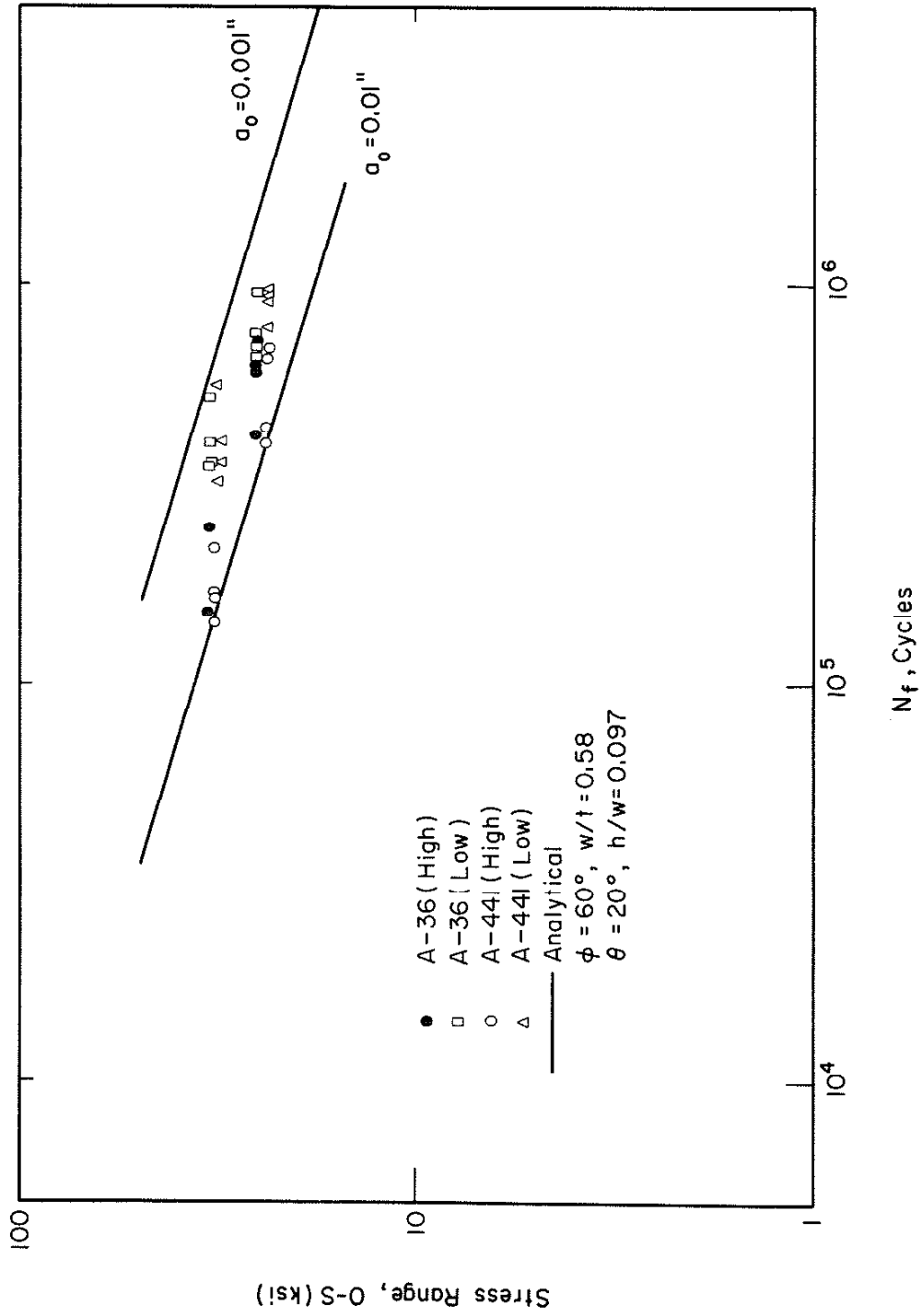


Fig. 16 Comparison of the Analytical and Test Results for the Fatigue Lives for A-36 and A-441 Steels

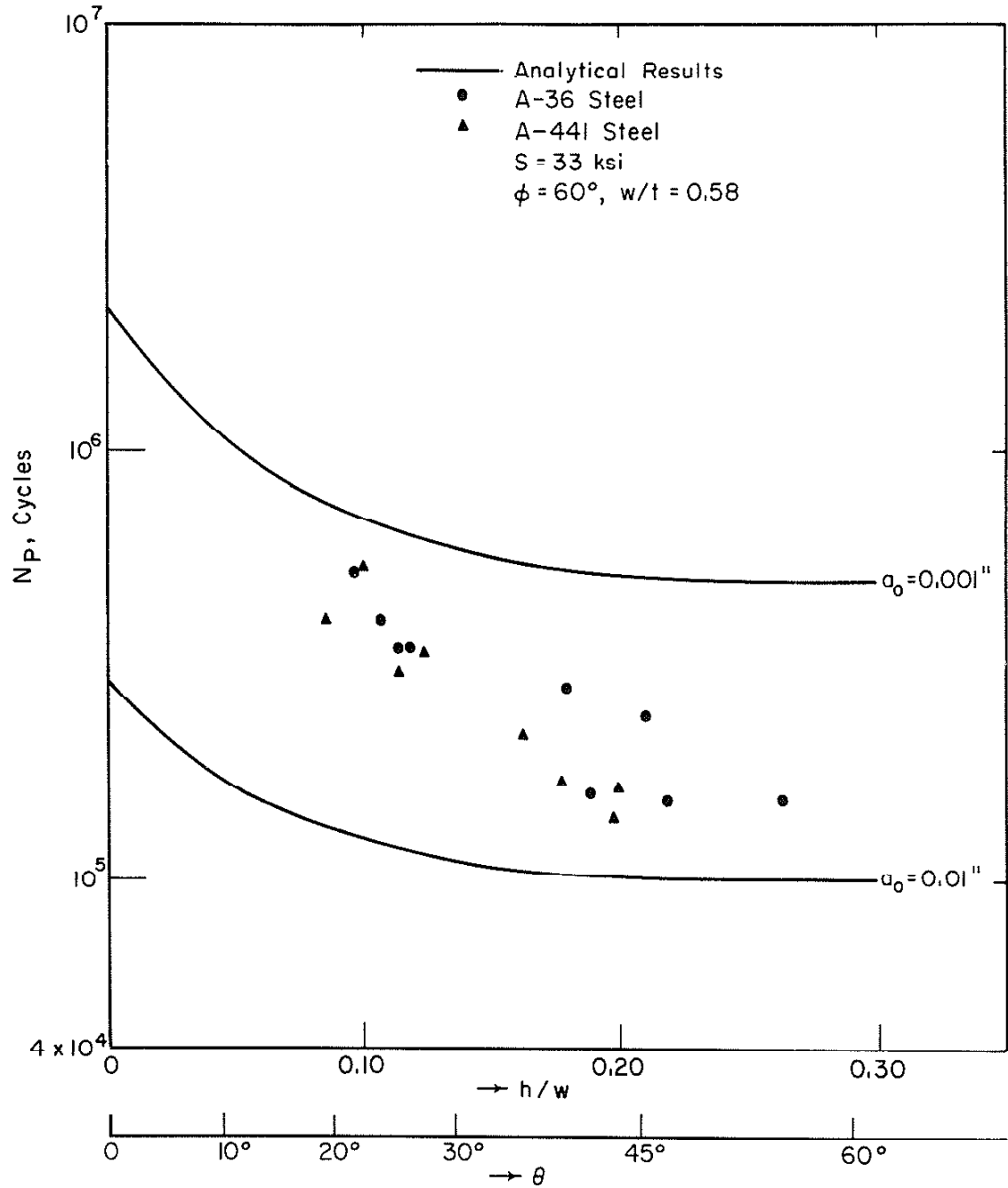


Fig. 17 Effect of Varying θ on Fatigue Lives of A-36 and A-441 Steels at a Stress of 0-33 ksi

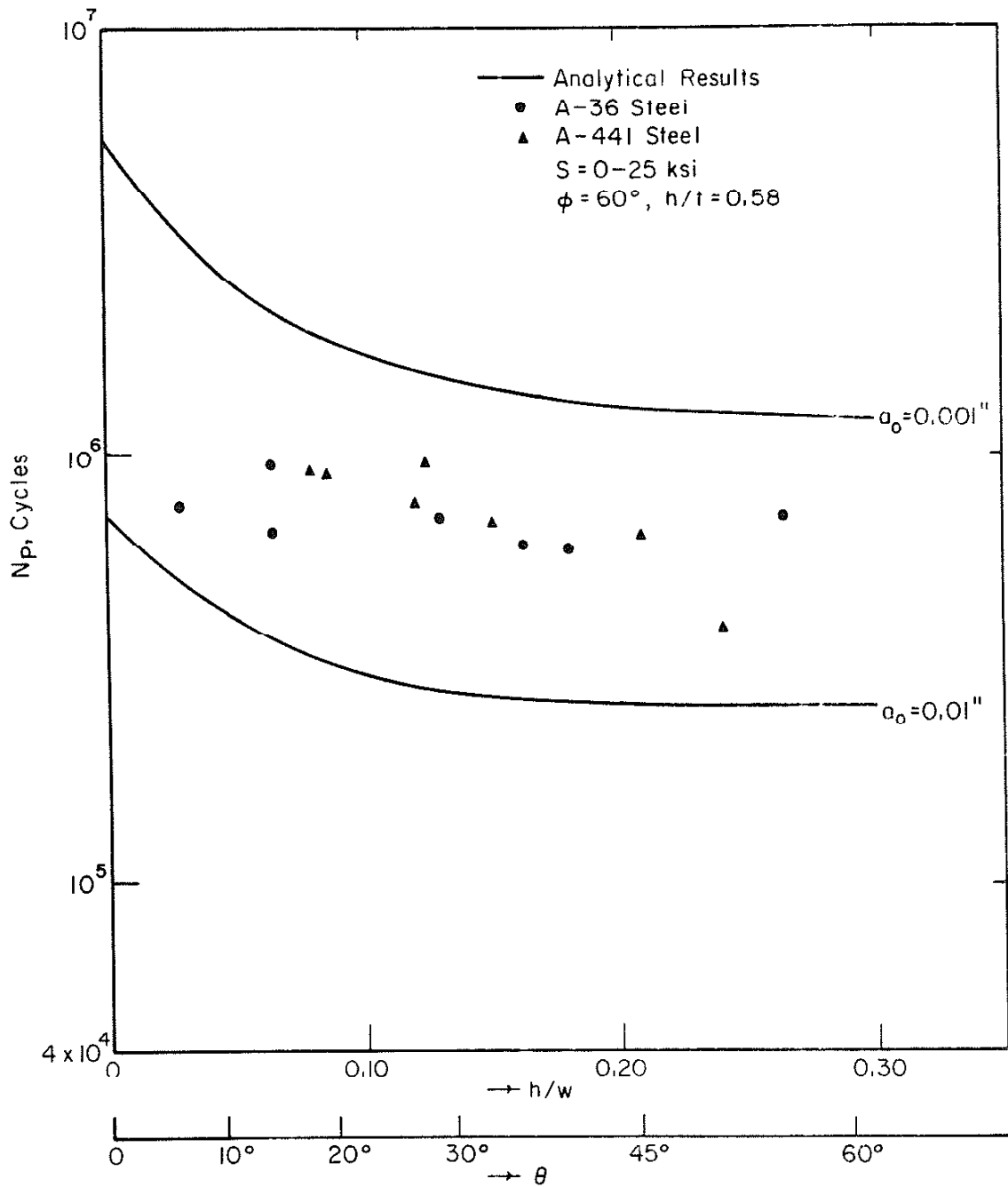


Fig. 18 Effect of Varying θ on Fatigue Lives for A-36 and A-441 Steels at a Stress of 0-25 ksi